ResearchGate

See discussions, stats, and author profiles for this publication at: https://www.researchgate.net/publication/275256644

Total ozone column, water vapour and aerosol effects on erythemal and global solar irradiance in Marsaxlokk, Malta

ARTICLE *in* ATMOSPHERIC ENVIRONMENT · DECEMBER 2014

Impact Factor: 3.28 · DOI: 10.1016/j.atmosenv.2014.10.005

CITATIONS
5

READS
30

5 AUTHORS, INCLUDING:

Roberto Román
Universidad de Valladolid
44 PUBLICATIONS **225** CITATIONS
SEE PROFILE

Charles Yousif
University of Malta
19 PUBLICATIONS **36** CITATIONS
SEE PROFILE

David Mateos
Universidad de Valladolid
47 PUBLICATIONS **309** CITATIONS
SEE PROFILE

Argimiro H De Miguel
Universidad de Valladolid
161 PUBLICATIONS **728** CITATIONS
SEE PROFILE

All in-text references underlined in blue are linked to publications on ResearchGate, letting you access and read them immediately.

Available from: David Mateos
Retrieved on: 26 January 2016

Atmospheric Environment 99 (2014) 508–518

Contents lists available at ScienceDirect

Atmospheric Environment

journal homepage: www.elsevier.com/locate/atmosenv

Total ozone column, water vapour and aerosol effects on erythemal and global solar irradiance in Marsaxlokk, Malta

Julia Bilbao [a, *], Roberto Román [a], Charles Yousif [b], David Mateos [a], Argimiro de Miguel [a]

[a] Valladolid University, Laboratory of Atmosphere and Energy, Faculty of Sciences, Valladolid, 47011, Spain
[b] University of Malta, Institute for Sustainable Energy, Marsaxlokk, 1531, Malta

HIGHLIGHTS

- Erythemal, global, diffuse and direct irradiances at Marsaxlokk, Malta.
- Ozone column, water vapour and aerosols influence on solar irradiances.
- Atmospheric compound effects and significance of irradiance changes.

ARTICLE INFO

Article history:
Received 10 June 2014
Received in revised form
1 October 2014
Accepted 4 October 2014
Available online 6 October 2014

Keywords:
Erythemal ultraviolet irradiance
Total solar shortwave irradiance
Total ozone column
Water vapour column
Aerosol
Central Mediterranean

ABSTRACT

Observations of erythemal (UVER; 280–400 nm) and total solar shortwave irradiance (SW; 305–2800 nm), total ozone column (TOC), water vapour column (w), aerosol optical depth (AOD) and Ångström exponent (α) were carried out at Marsaxlokk, in south-east Malta. These measurements were recorded during a measurement campaign between May and October 2012, aimed at studying the influence of atmospheric compounds on solar radiation transfer through the atmosphere. The effects of TOC, AOD and *w* on UVER and SW (global, diffuse and direct) irradiance were quantified using irradiance values under cloud-free conditions at different fixed solar zenith angles (SZA). Results show that UVER (but not SW) irradiance correlates well with TOC. UVER variations ranged between −0.24% DU^{-1} and −0.32% DU^{-1} with all changes being statistically significant. Global SW irradiance varies with water vapour column between −2.44% cm^{-1} and −4.53% cm^{-1}, these results proving statistically significant and diminishing when SZA increases. The irradiance variations range between 42.15% cm^{-1} and 20.30% cm^{-1} for diffuse SW when SZA varies between 20° and 70°. The effect of aerosols on global UVER is stronger than on global SW. Aerosols cause a UVER reduction of between 28.12% and 52.41% and a global SW reduction between 13.46% and 41.41% per AOD550 unit. Empirical results show that solar position plays a determinant role, that there is a negligible effect of ozone on SW radiation, and stronger attenuation by aerosol particles in UVER radiation.

© 2014 Elsevier Ltd. All rights reserved.

1. Introduction

The ultraviolet (UV) solar range contains the most energetic wavelengths of the total solar shortwave (SW) radiation that reaches the Earth's surface, and is involved in photochemical reactions and photobiological processes that take place in the atmosphere and the biosphere, respectively. UV radiation affects human health (both short-term deterministic effects, such as erythema or sunburn, and long-term deterministic/stochastic effects such as photoaging/skin cancer), damages aquatic life, affects plants, affects conservation and durability of materials, in addition to impacting global energy balance and climate change (UNEP, 2010). Yet, not all effects are harmful, with synthesis of vitamin D being one of the beneficial effects of UV (Webb, 2006; Fioletov et al., 2009). Different action spectra are used to quantify these effects. McKinlay and Diffey (1987) established the erythemal action spectrum, which represents the spectral response of human skin to UV radiation able to trigger an erythema (or sunburn). The solar radiation weighted with this spectrum is called erythemal radiation (UVER; 280–400 nm) (Webb et al., 2011; C.I.E. 1998).

Ultraviolet solar radiation in the lower atmosphere and at the Earth's surface has been widely studied in recent decades due to the above-mentioned influence on the atmosphere and on living beings. Different studies show that clouds, ozone and atmospheric

* Corresponding author.
E-mail address: juliab@fa1.uva.es (J. Bilbao).

http://dx.doi.org/10.1016/j.atmosenv.2014.10.005
1352-2310/© 2014 Elsevier Ltd. All rights reserved.

aerosols are the atmospheric compounds that mainly attenuate UV reaching the surface (WMO, 2010). UVER solar radiation is attenuated by stratospheric and tropospheric ozone absorption which depends on wavelength. The influence of TOC on UV radiation is highly wavelength-dependent, UV-A radiation (315–400 nm) is scarcely attenuated by ozone and UV-B (from 280 to 315 nm, approximately) is significantly affected by changes in ozone.

Various authors have researched into the TOC influence on UV. McKenzie et al. (1991) showed the relationship between UVER and ozone, and found that an ozone reduction of 1% leads to a 1.25 ± 0.20% increase in UVER irradiance. Koepke et al. (2002) showed that UVER dependence on TOC varies with the solar zenith angle (SZA). Seckmeyer et al. (1997) and Stick et al. (2006) observed ozone changes over shorter time scales whose impact on UV changes may also prove important. Siani et al. (2002) studied the effect of low ozone episode on ultraviolet solar radiation for the Mediterranean area. Antón et al. (2008) analysed the influence of short-term changes in TOC on UVER in south-west Spain, and reported that low-ozone events in winter cause a 30% increase in UVER. De Miguel et al. (2011) found that UVER changes with TOC at the rate $-0.35 \pm 0.03\%\ DU^{-1}$ for SZA values near 65° in central Spain.

Aerosols are atmospheric particles can affect incoming solar radiation directly by absorption and scattering, and indirectly acting as cloud condensation nuclei (modifying cloud microphysical properties). Both effects contribute to cooling the Earth's surface and simultaneously warming the lower atmosphere (Pace et al., 2006).

Aerosol effects on UV irradiance have been studied by several authors, through both field observations and radiative transfer model calculations. Liu et al. (1991) showed the effect of anthropogenic aerosols on UVER and observed a reduction of between 5% and 18% at ground level that may have been balanced by the increase in UV due to stratospheric ozone depletion. Changes in aerosol size and absorption properties over the year cause significant effects, such that mineral aerosol load might reduce (~25%) UVER solar irradiance at surface when aerosol optical depth increases by one unit for SZA below 25° (Antón et al., 2011). Kazadzis et al. (2009) obtained the aerosol optical depth (AOD) at 340 nm from spectral irradiance measurements at Thessaloniki, Greece, and reported a 15% reduction in UV irradiance in the 325–340 nm range for a unit of aerosol optical depth.

Using measurements and models, Esteve et al. (2009) estimated the influence of ozone and aerosols on UVER solar radiation in Valencia, Spain and found that 70% of the variation in UVER is explained by the variation in ozone and aerosols. Badarinath et al. (2007) report that tropospheric aerosol loading on UVER has a significant impact in a tropical area of Hyderabad, India and that UVER decreases by 24% on days with high aerosol load.

Certain studies into this topic are based on radiative transfer models, such as the work of Meloni et al. (2003) who used measurements from a spectroradiometer and a radiative transfer model, and reported a 12.5% and 16.7% reduction in UV over two days of study. Román et al. (2013) described the effects of a desert dust episode at Granada (Spain) on global, direct and diffuse spectral UV irradiance, finding that attenuation of direct UV was about 50% while diffuse irradiance increased by up to 40%. Papadimas et al. (2012) computed the direct radiative effect of natural plus anthropogenic aerosols on the solar radiation budget. Theirs was the first study to focus on the entire Mediterranean area and to compute all aerosol effects separately, their study revealing significant atmospheric warming and surface radiative cooling.

In addition, to study the role of ozone and aerosols on the transfer of ultraviolet and visible radiation through the atmosphere, the Photochemical Activity and Ultraviolet Radiation modulation factor campaign (PAUR II) took place at Lampedusa (Italy), an island in the Mediterranean (Di Sarra et al., 2002). Results indicated a 20% reduction in UV irradiance at 350 nm at a solar zenith angle of 30° and a 25% reduction at 60° caused by increased desert dust aerosols.

Due to the major impact which desert dust and other factors have on solar radiation and in order to ascertain solar UVER irradiance and atmospheric compound levels in a Mediterranean area, a measurement campaign was established at Marsaxlokk (Malta) from May to October 2012, following the recommendations of UNEP (2010). The aim of the campaign was to measure, for the first time to the best of our knowledge, atmospheric compounds such as aerosols, ozone and water vapour, as well as UVER and SW (global, direct and diffuse) irradiance, in the Central Mediterranean area.

The present paper seeks to analyse the influence and effects of the total ozone column, water vapour column (w), aerosol optical depth, and Ångström exponent (α) on UVER and global, diffuse and direct SW irradiance. This paper thus contributes to improving the understanding and quantification of the influence of atmospheric compounds on UVER and global solar irradiance in Malta. The interest of the study is based on the strong interactions between ozone depletion and climate change in addition to uncertainties in the measurements and models which limit our confidence in predicting future UV and total radiation. It is therefore important to improve our understanding of the processes involved, and to continue monitoring ozone and surface UV spectral irradiances both from surface and from satellites so that we can respond to unexpected changes in the future (UNEP, 2010). Results and analysis should also contribute to increase our knowledge of the atmospheric variables which shape the influence of the atmosphere on solar radiation variability by its relation with solar energy applications (Gueymard, 2012).

In the following sections, the site description, instrument and data collection are detailed, the methodology is explained, the observations and results are analysed in relation with the influence of SZA, TOC, water vapour column, AOD at 550 nm (AOD_{550}) and Ångström exponent on UVER irradiance and in the components of SW irradiance: global (SW_{glo}), diffuse (SW_{dif}), and direct (SW_{dir}). The most interesting conclusions are given in the final section.

2. Instrumentation and data

2.1. Measurement site

The measurement campaign took place at Marsaxlokk, a village located in a rural area close to the Mediterranean sea in south-east Malta about 20 km from the city of Valetta, Malta. The region's climate is influenced by Mediterranean air masses, and local weather is usually warm in summer with temperatures of 30 °C and high humidity. In winter, the weather is not too cold, only when air masses come from the north and northeast (central Europe). In fact, daytime winter temperatures almost never fall below 10 °C.

The campaign involved two European Institution Groups: the Institute for Sustainable Energy at the University of Malta, and the Atmosphere and Energy Laboratory at the University of Valladolid, Spain. Solar radiation instruments used for this study were located on the rooftop of the Institute for Sustainable Energy (35.84°N; 14.54°E; 10 m a.s.l.) which had an obstruction-free horizon.

2.2. Ground-base instruments

UVER and SW (global, diffuse and direct) irradiance were measured by pyranometers, total ozone column, water vapour column and aerosol optical depth were retrieved from satellite remote sensing and Ångström exponent was obtained from

Lampedusa, Aeronet station. A Solar Light Microtops-II manual Sun photometer (of the Valladolid University) was used throughout the campaign to obtain TOC and AOD at 1020 nm.

UVER measurements were recorded using a UVB-1 pyranometer (Yankee Environmental Systems) that has a spectral response similar to the erythemal action spectrum. Pyranometer sampling rate was 10 s but these are averaged and recorded every 1 min and every 10 min; as a result we have 10-min UVER measurements. The raw signal of the instrument was converted into erythemal units by calibration coefficients which depend on SZA and TOC. The calibration coefficients were calculated just after the campaign at the National Institute for Aerospace Technology (Huelva, Spain), following the method of Vilaplana et al. (2009). The combined uncertainty of the UVER measurements obtained in this way ranges between 5.6% and 8% depending on the cosine response (Hülsen and Gröbner, 2007). Mateos et al. (2014a,b) found that differences between UVER values from UVB-1 and UVER values from the Brewer spectrometer were below 5%. More details concerning the quality control of UVB-1 data can be found in Bilbao et al. (2004, 2011) and Mateos et al. (2013).

Global and diffuse SW irradiance were recorded by two CM21 (Kipp & Zonen) pyranometers, one of which was equipped with a shadow-band. Diffuse solar irradiance data were corrected following the proposed method by Batlles et al. (1995) and Perez et al. (1990) that take into account geometric and atmospheric (clearness index) corrections. Global and diffuse irradiance pyranometer sampling rates were 10 s but these are averaged and recorded every 1 min and every 10 min; as a result we have 10-min SW irradiance measurements. The CM21 (Kipp & Zonen) instruments have a flat spectral response from 305 to 2800 nm and the cosine effect is less than 3% for solar elevation above 10°. CM21 sensors are regularly calibrated by comparison with a reference sensor at Kip & Zonen manufacturer and the differences obtained in percentage are lower than 2%.

SW_{dir} irradiance was evaluated from global and diffuse solar components:

$$SW_{dir} = SW_{glo} - SW_{dif} \quad (1)$$

The pyranometers were connected to a Campbell CR23X data logger, which was programmed to take measurements each 10s and to compute average global and diffuse irradiance values each one and ten minutes (Bilbao and de Miguel, 2013).

A Solar Light Microtops-II manual Sun photometer (of the Valladolid University) was used throughout the campaign to measure TOC and AOD at 1020 nm. The Sun photometer Microtops-II is equipped with five optical collimators, with a field of view of 2.5°, to perform direct radiation measurements at the following nominal wavelengths: 305, 312, 320, 936, and 1020 nm. The instrument was calibrated each two years at the Mauna Loa Observatory (Hawaii) and in the Solar Light Calibration Lab (Glenside, PA). Furthermore, an inter-comparison of ozone data between this Microtops-II and the Brewer spectrometer was carried in Lampedusa island (Central Mediterranean) exhibiting root-mean-square differences below 1% (Mateos et al., 2014b). More details about solar irradiance sensors are given by De Miguel and Bilbao (2005).

2.3. Satellite-borne instruments

During the campaign, whenever Microtops TOC measurements were not available because of cloudy conditions, data from the Ozone Monitoring Instrument (OMI; onboard Aura satellite) were used. If TOC from OMI was not available, data from the Global Ozone Monitoring Experiment-2 instrument (GOME-2; onboard MetOp-A satellite) were used. These satellite-based data were obtained from the Aura Validation Data Center (AVDC: http://avdc.gsfc.nasa.gov) as overpass files. The TOC from OMI retrieved by the TOMS (OMI_{TOMS}) and DOAS (OMI_{DOAS}) algorithms, and the TOC retrieved from GOME-2 (GOME2) were compared with Microtops measurements, and showed a high correlation between ground-based and satellite-based TOC for the three databases. OMI_{TOMS} was seen to be the most similar TOC data series to ground measurements followed by OMI_{DOAS} and then GOME-2. The correlations obtained between sun photometer and satellite TOC and AOD_{1020} retrieval daily values are shown and compared in Table 1. Also, a correlation coefficient between OMI and Microtops-II TOC daily data of 0.95 was obtained during a two month campaign in Southern Italy, Mateos et al. (2014a).

Water vapour column data were also obtained from the noon measurements of the MODIS instrument (Moderate Resolution Imaging Spectroradiometer) on board the Terra satellite, using MODIS infrared channels. Román et al. (2014) compared this MODIS product against ground-based water vapour measurements in a Mediterranean region, and found that the combined uncertainty of MODIS water vapour increases from 0.38 cm to 0.52 cm when water vapour increases from 0.5 cm to 3 cm.

The AOD_{550} was also obtained from the MODIS instrument and was considered as constant daily values. Uncertainty in the AOD_{550} from MODIS was expected to be 0.05 plus 20% of the retrieved AOD_{550} (Kaufman et al., 1997). Ångström exponent values were also obtained from Aeronet (http://aeronet.gsfc.nasa.gov/new_web/index.html) daily data at the nearest Italian station at Lampedusa (35.52°N; 12.63°E; 45 m a.s.l.) (Meloni et al., 2003). When AOD_{550} from MODIS were not available, it was calculated using the Ångström exponent and the AOD at 1020 nm from Microtops-II. The MODIS data used in this work were downloaded from the GIOVANNI application (http://disc.sci.gsfc.nasa.gov/giovanni/overview/index.html) as the value average in a 0.2° side square, whose centre is at the Institute for Sustainable Energy, Marsaxlokk, Malta.

2.4. Data analysis

Measurements of solar irradiance and atmospheric compounds were analysed using the software package "MATLAB Corrcoef" function (www.mathworks.es). The significance of the correlation coefficients, r, was tested at the confidence level of 99% and significance level of 0.01 The p-value was used in the context of null hypothesis testing to quantify the statistical significance of r. If the p-value is less than the significance level the null hypothesis is rejected and the correlation coefficient is significant. For this proposal the p-value is evaluated using the t-distribution with $n - 2$ degrees of freedom, n being the number of data. In addition, the lower and upper bounds for each coefficient r at 99% confidence level have been evaluated. The calculations are based on the Fisher transformed defined by: $z = 0.5 \log [(1 + r)/(1 - r)]$ and the standard deviation being $1/\sqrt{n - 3}$; the Fisher transformed and its inverse have been used to construct the confidence intervals for r, (Román et al., 2012).

Table 1
Comparison of total ozone column and AOD_{1020} values from Microtops II and satellite retrievals, for the period May to October 2012 at Marxaslokk, Malta.

TOC (DU)	r	MBE (%)	RMSE (%)	σ (DU)
Microtops II(DU) – OMI-TOMS	0.95	−0.12	1.5	4.5
Microtops II (DU) – OMI-DOAS	0.86	−0.66	2.5	7.6
Microtops II (DU) – GOME-2	0.95	−0.66	1.7	4.7
AOD1020-MICROTOPS – II	r	MBE (%)	RMSE (%)	σ
Microtops II AOD1020 – MODIS	0.70	0.03	0.06	0.06

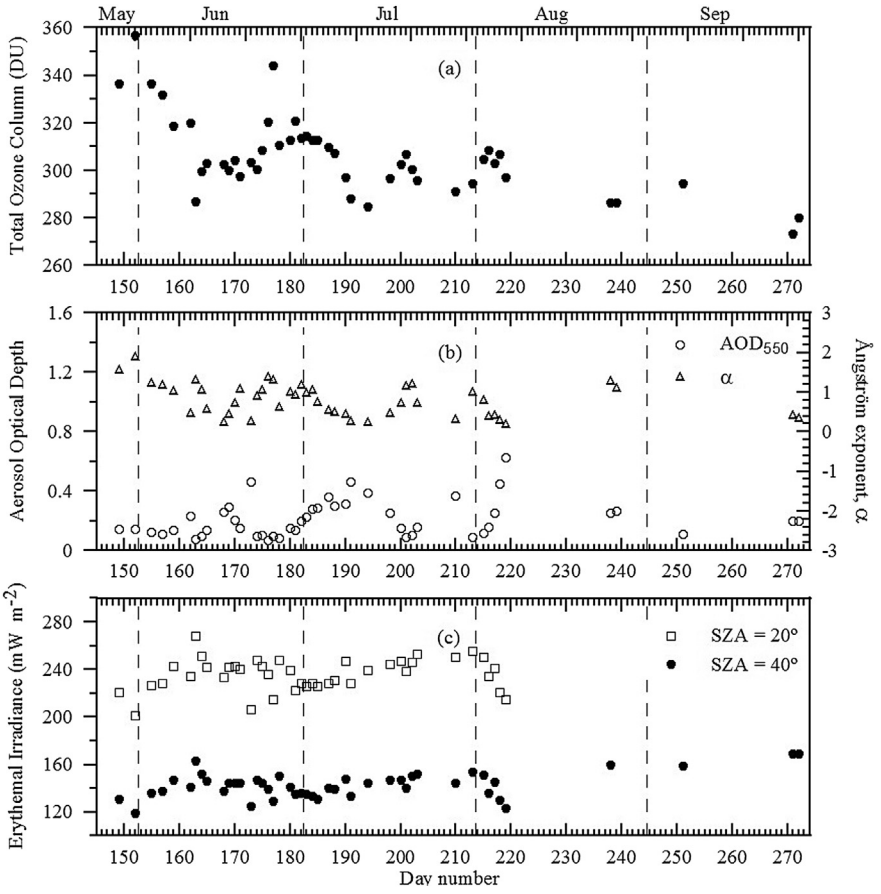

Fig. 1. Evolution under cloudless conditions of a) daily total ozone column, TOC (solid circles); b) aerosol optical depth at 550 nm, AOD_{550nm} (open circles) and Ångström exponent, α, (open triangles); c) erythemal irradiance at solar zenith angles of 20° (open squares) and 40° (solid circles for the period May to October 2012 at Marxaslokk, Malta.

3. Methodology

In order to evaluate the effect of different atmospheric compounds on UVER and SW solar irradiance, only measurements performed in clear sky conditions were used. The selection of clear sky days was based on a visual inspection (using 1-min values) of the radiometer daily curves of SW (global, diffuse and direct) and UVER. Possible uncertainties of using this method are those situations with clouds not close to the Sun, because the radiative field is not changed enough. However, the fast scan (1-min) minimizes their impact on our method. After the representation and observation of the daily curve evolutions, days classified as cloudless sky were retained and used for the analysis. As a result, a total of 47 days are identified as entirely cloud-free.

The method described in the following was applied to estimate the impact of total ozone, aerosols and water vapour on ultraviolet and visible irradiance at surface.

3.1. Earth-sun distance normalization

In order to remove dependence on astronomical factors, cloudless data were normalized to the Earth-Sun distance (ESD) of

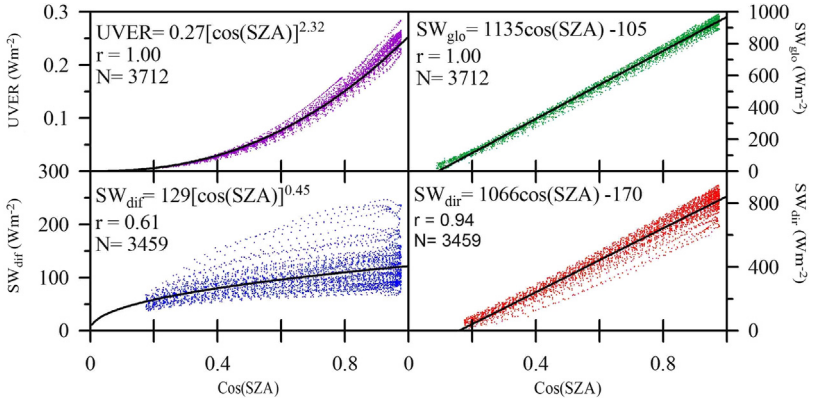

Fig. 2. UVER (up left), SW_{glo} (up right), SW_{dif} (down left) and SW_{dir} (down right) normalized to 1 (AU) as a function of solar zenith angle, SZA, and cloudless conditions, during the period May to October 2012 at Marxaslokk, Malta. Black lines correspond to lineal fits (for SW_{glo} and SW_{dir}) and potential fits (for UVER and SW_{dif}). Number of data, the fit equation, and correlation coefficients are included.

1AU (Astronomic Unit) dividing the irradiances by the eccentricity of the Earth-sun orbit (ε), calculated by the following expression (Iqbal, 1983):

$$\varepsilon = 1 + 0.033\cos\left(\frac{2\pi d_n}{365}\right) \quad (2)$$

where d_n is the number of the day.

3.2. SZA normalization

The SZA was calculated each minute by the algorithm of Reda and Andreas (2003), and the SZA assigned to a 10-min (UVER or SW) measurement was the average of the ten values of SZA over the 10 min. In order to remove the SZA effect on UVER and SW irradiance, measurements were only selected (under cloudless conditions) if their assigned SZA value was (within ±0.5°) one of the considered SZA of reference: 15°, 20°, 25°, 30°, 35°, 40°, 45°, 50°, 55°, 60°, 65° or 70°. The selected irradiance values were normalized to the reference SZA (SZA_R) multiplying the irradiance by the next factor (F_{SZA}):

$$F_{SZA} = \frac{\cos(SZA_R)}{\cos(SZA)} \quad (3)$$

This provided 12 different datasets, one per each SZA mentioned. In this work, the corresponding irradiance measurements are plotted as a function of the atmospheric components although only 6 of the 12 data series are shown on the figures for clarity.

3.3. Statistical analysis

In order to analyse the influence of atmospheric components on solar irradiance, UVER and SW (global, diffuse and direct) irradiance were plotted as a function of different atmospheric components (TOC, w, AOD_{550} and α) for each SZA of reference and the linear regression fits were applied. For each SZA interval and compound, the fit slope (b), solar irradiance percentage change (B), correlation coefficient (r), p-value and the 99% confidence interval of r (i99%) were evaluated. The percentage change was considered as the ratio between the fit slope and the solar irradiance (UVER or SW) averaged using the fit data. The last value was multiplied by 100% to obtain the unit in % per unit of the atmospheric compound as can be seen in the following expression:

$$B = 100\%\frac{b}{\bar{I}_y} \quad (4)$$

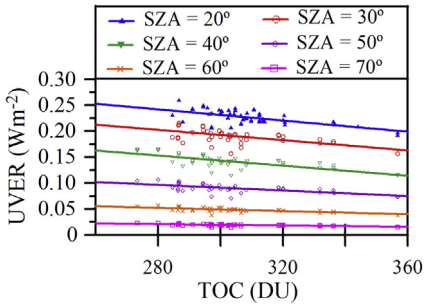

Fig. 3. UVER irradiance as a function of the total ozone column, TOC, for different solar zenith angles, SZA, and cloudless conditions, during the period May to October 2012 at Marxaslokk, Malta.

where b is the fit slope obtained by the least squares method. B is the percentage change defined as the percentage variation caused in UVER and SW irradiance due to a unit change in atmospheric compound and $\bar{I}_y$ is the average of values of the irradiance used in each regression. B values were obtained using the slope b obtained by linear fits of each fixed solar zenith angles. The radiation amplification factor (RAF), which represents the percent that changes the irradiance by 1% of change in the atmospheric compound (McKenzie et al., 1991), was also calculated using the method explained by De Miguel et al. (2011): a linear method which calculates RAF multiplying B by the average (divided by 100%) of the atmospheric compound used in the fit.

The p-value and the correlation coefficient and its 99% confidence interval were the three parameters used to explain the statistical significance of the fits. If the p-value is smaller than the significance level (in our case 0.01), then the fit can be considered statistically significant (in our case at 99% confidence level). Statistically significant fits were also identified calculating the 99% confidence interval and the standard error for the correlation coefficient r. In this study, a fit was considered statistically significant at 99% when the standard error of r (99% confidence) is below the absolute value of r. A similar method was used by De Miguel et al. (2011).

4. Observations and results

First, Fig. 1 shows the temporal evolution of daily total ozone column, aerosol optical depth at 550 nm, Ångström exponent, and cloudless UVER irradiance at solar zenith angles of 20° and 40°. The total ozone column average value was 306 DU and this varies by about ±42 DU around the average value, the variability interval being around ±14%. A maximum TOC value on a cloudless day was obtained on 31 May 2012 with 356 DU and the minimum was 273 DU on 27 September 2012.

Aerosol optical depth at 550 nm on a cloudless day varies between 0.03 (19 July 2012) and 0.63 (6 August 2012), and the variability interval is ±98% indicating that extremely different atmospheric aerosol conditions may occur. This variability can be expected to produce significant variations in the measured UV irradiances. In this way, AOD_{550} frequently shows values above 0.3 during the campaign which can have an important effect on radiative transfer through the atmosphere (Di Sarra et al., 2001). The Ångström exponent on a cloudless day ranges between 0.22 (6 August 2012) and 1.92 (31 May 2012), low AOD values usually corresponding to high Ångström exponent values. Fig. 1 shows that for large AOD values, the Ångström exponent values are close to 0.5, these being low values related to coarse particles like Saharan desert dust (Román et al., 2013).

Fig. 1 also shows that for low total ozone column values, the UVER displays larger values. However, significant anomalies may sometimes be observed. Fig. 1 shows that low UVER values are recorded for total ozone column below 300 DU. For example, 9 July when UVER decreased and TOC was 288 DU might have been due to changes in aerosol content that contribute towards explaining the variability of UVER irradiance (in fact, a desert dust event, not shown here, occurred on this day). Similar significant UV anomalies were also observed by Di Sarra et al. (2002) at Lampedusa during the PAUR II campaign, these probably being caused by changes in aerosol content.

4.1. SZA effect

In order to evaluate the influence of SZA on UVER and SW (global, diffuse and direct) irradiance, these irradiances measured under cloud-free conditions are represented as a function of the

Table 2
Number of data, *N*, SZA(°), fit slope, *b* (Wm^{-2} DU^{-1}), percentage change, *B* (%DU^{-1}), RAF, correlation coefficient *r*, *p*-value, and 99% confidence interval obtained for the UVER irradiance as functions of TOC, for different SZA values, for the period May to October 2012 at Marxaslokk, Malta.

Irradiance	*N*	SZA	*b* (Wm^{-2} DU^{-1})	*B* (% DU^{-1})	RAF	*r*	*P*	i99%
UVER	63	20	−0.0006	−0.24	0.76	−0.62	<0.001	(−0.787, −0.378)
	45	30	−0.0005	−0.26	0.78	−0.56	<0.001	(−0.774, −0.232)
	44	40	−0.0005	−0.34	1.04	−0.73	<0.001	(−0.870, −0.483)
	41	50	−0.0003	−0.30	0.91	−0.62	<0.001	(−0.818, −0.304)
	39	60	−0.0002	−0.31	0.95	−0.62	<0.001	(−0.821, −0.294)
	37	70	−0.0001	−0.32	0.98	−0.59	<0.001	(−0.808, −0.232)

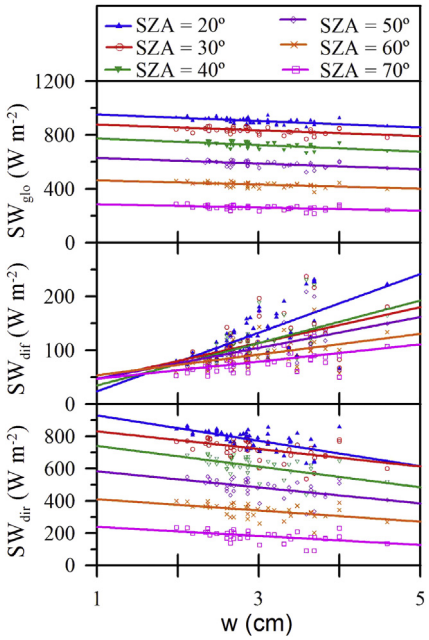

Fig. 4. SW_{glo} (up), SW_{dif} (middle) and SW_{dir} (bottom) irradiances under cloudless conditions as a function of water vapour column for three different solar zenith angles, during the period May to October 2012 at Marxaslokk, Malta.

cosine of SZA (for all SZA values below 85°) in Fig. 2. This figure shows the analytic relation between the irradiances with SZA cosine and, as expected, UVER fits as a power function and SW_{glo} fits as a linear behaviour. The reason for this behaviour is caused by the ratio between diffuse and direct components. Similar fits were obtained by Dubrovsky (2000) and Román et al. (2012).

Direct SW irradiance on a horizontal surface represented in Fig. 2 shows a linear behaviour except for high SZA values. The lowest values for each SZA are due to the presence of high aerosol load. The linear behaviour indicates that the atmosphere transmittance for SW irradiance does not exhibit significant variations with SZA since the direct component follows a cosine law. However, diffuse SW irradiance (low panel) shows a different function with SZA, similar to a power function, the highest values being due to high aerosol load episodes. The diffuse component is much lower than the direct component in SW_{glo} irradiance, making the behaviour of global SW linear. The opposite happens in global UVER, whose behaviour is similar to diffuse SW.

4.2. Total ozone column effect

TOC influences UV due to its absorption bands at this range. To observe the effect of atmospheric compounds on UVER radiation, the SZA effect was removed from the data series. Twelve subsets were chosen following the method used in Section 3.2. These data series are plotted as a function of TOC for different SZA intervals in Fig. 3 and their regression lines are also included (only six different datasets are shown for clarity). UVER irradiance can be seen to decrease when TOC increases.

The results are summarized in Table 2 which shows the UVER irradiance data number, the fit slope in energy and percentage per Dobson unit, the radiation amplification factor estimator, the correlation coefficient of the fits and its i99%, and the probability *p*-value. UVER shows negative fit slopes that are significant at the 99% level with *p*-values below 0.001; the UVER percentage variation decrease from −0.24% DU^{-1} to −0.32% DU^{-1} and rise from −30% DU^{-1} to −0.26% DU^{-1} when SZA ranges between 20° and 45° and from 50° to 65° respectively; the average variation being −0.31% DU^{-1}. A similar result, −0.35% DU^{-1} was obtained by De Miguel et al. (2011) using UVER monthly averages in central Spain. RAF values range between 0.76 and 1.04 depending on SZA; RAF values are smaller than those reported in early publications (Madronich et al., 1998; De Miguel et al., 2011); correlation coefficients are negative, and range between −0.56 and −0.73 for different SZA.

4.3. Water vapour column effect

The water vapour column effect was studied on global SW irradiance and also on its diffuse and direct components, but not in UVER since *w* has no absorption bands in the UV range. Fig. 4 shows SW_{glo}, SW_{dif} and SW_{dir} as a function of *w* for different SZA values. SW_{glo} and SW_{dir} diminish when *w* increases and SW_{dif} increases with *w*. Results are summarized in Table 3. The percentage variations obtained for global SW are between −2.44 and −4.53 (% cm^{-1}) and are greater when SZA is higher. All results are significant with *p*-values below 0.001. Direct SW irradiance changes are also statistically significant, with SW_{dir} decreasing when *w* rises. The diffuse component shows a statistically significant positive correlation that increases when the water vapour column rises, the maximum being for SZA 20°.

However, this does not have much sense since the only water vapour column effect on solar radiation is by absorption, and the increase in solar diffuse could only occur if water vapour produced scattering (which is not the case). This means that the correlation between SW_{dir} and *w* does not imply causation. Diffuse SW thus increases with the water vapour column since the water vapour is also correlated (no causation) with aerosol optical depth (plot not shown) and, as a consequence, Fig. 4 (middle) shows the increases in SW_{dif} due to a rise in aerosol load.

The correlation between *w* and AOD_{550} might be related to dust episodes in Malta whose synoptic conditions also increase water vapour. The following remarks explain the hypothesis because it has been observed that SW_{dif} does not increase with *w* when AOD_{550} is fixed (Figure not shown); also backward trajectories from desert http://ready.arl.noaa.gov/HYSPLIT.php, (not shown) were observed for days with high water vapour *w* joined to west component winds (Sicily sounding station, http://weather.uwyo.

Table 3
Number of data, *N*, SZA(°), fit slope, *b* (Wm^{-2} cm^{-1}), percentage change, B (% cm^{-1}), correlation coefficient *r*, *p*-value, and 99% confidence interval obtained for the SW_{glo}, SW_{dif}, SW_{dir}, irradiances as functions of *w*, for different SZA values, for the period May to October 2012 at Marxaslokk, Malta.

Irradiance	N	SZA	*b* (Wm^{-2} cm^{-1})	*B* (% cm^{-1})	*r*	*p*	i99%
SW_{glo}	63	20	−24	−2.44	−0.56	<0.001	(−0.748, −0.295)
	45	30	−22	−2.48	−0.50	0.001	(−0.737, −0.147)
	44	40	−25	−3.22	−0.51	<0.001	(−0.749, −0.165)
	41	50	−22	−3.45	−0.51	<0.001	(−0.754, −0.146)
	39	60	−16	−3.49	−0.48	0.002	(−0.741, −0.095)
	37	70	−13	−4.53	−0.45	0.006	(−0.727, −0.039)
SW_{dif}	63	20	58	42.15	0.63	<0.001	(0.390, 0.792)
	45	30	36	29.64	0.50	0.001	(0.145, 0.735)
	44	40	42	35.57	0.56	<0.001	(0.221, 0.774)
	41	50	31	27.36	0.48	0.001	(0.107, 0.737)
	39	60	21	20.95	0.43	0.006	(0.037, 0.714)
	37	70	17	20.30	0.50	0.002	(0.106, 0.757)
SW_{dir}	63	20	−82	−9.93	−0.63	<0.001	(−0.791, −0.387)
	45	30	−58	−7.50	−0.51	<0.001	(−0.745, −0.165)
	44	40	−67	−10.27	−0.55	<0.001	(−0.772, −0.218)
	41	50	−52	−10.18	−0.51	0.001	(−0.751, −0.139)
	39	60	−37	−10.15	−0.47	0.003	(−0.733, −0.076)
	37	70	−30	−15.41	−0.49	0.002	(−0.753, −0.097)

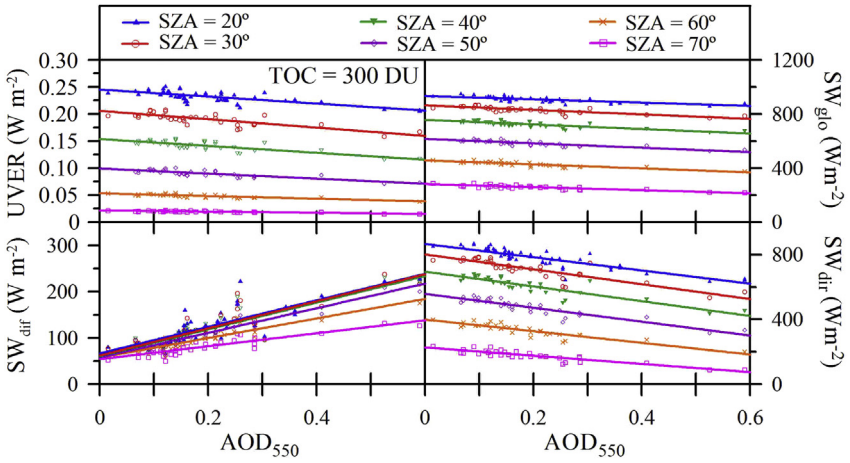

Fig. 5. UVER irradiance normalized to 300 DU (top left), SW_{glo} (top right), SW_{dif} (bottom left) and SW_{dir} (bottom right) under cloudless conditions as a function of aerosol optical depth at 550 nm for different SZA values, during the period May to October 2012 at Marxaslokk, Malta.

edu/upperair/sounding.html), therefore the dust episodes in Malta whose synoptic conditions also increase water vapour make possible the hygroscopic growth of aerosols and as consequence the increases of SW_{dif}. In conclusion, there are correlations between SW irradiance components and water vapour column, although variations might actually be higher than what water vapour column really affects since the effect of aerosol is also implicit on variations.

4.4. Aerosol optical depth effect

In order to evaluate the aerosol effect on UVER, TOC influence was removed by normalising UVER irradiance to 300 DU using the following expression (Román et al., 2012):

$$UVER_{300\ DU} = \left(1 - B_{O_3}\frac{300 - TOC}{100}\right)UVER \quad (5)$$

where $UVER_{300DU}$ is the UVER irradiance normalized to 300 DU, B_{O_3} is the percentage change in UVER evaluated in Table 2 (which is a function of the solar zenith angle), TOC is the measured total ozone column, and UVER is the measured irradiance value. Global, diffuse and direct SW were not normalized for the water vapour value because the aerosol effect is just implicit on the changes, as observed in the previous section.

Fig. 5 shows the UVER, SW_{glo}, SW_{dif} and SW_{dir} solar irradiances as a function of aerosol optical depth at 550 nm for different solar zenith angles. It can be observed that SW_{dif} increased with AOD_{550} and that UVER, SW_{glo} and SW_{dir} diminished when AOD_{550} increases.

It can be observed in Table 4 that all percentage changes for UVER, SW_{glo}, SW_{dif} and SW_{dir} are statistically significant at 99% confidence level. The effect of aerosol on UVER irradiance increases when SZA increases, the percentage variations values being located in the interval −28.1 to −52.4% per AOD_{550} unit. Román et al. (2012) found an average change value of −37% by one unit of AOD at 440 nm in UVER irradiance, at central Spain in agreement with the present results.

Percentage change on SW caused by AOD_{550} can be implicitly influenced by water vapour column, although in SW_{dif} they would have no effect (water vapour does not scatter SW, at least significantly). Changes increase in absolute value with SZA for SW_{glo} and SW_{dir}, contrary to SW_{dif}, whose changes are higher when SZA diminishes. SW_{glo} changes range between −13.5% and −41.4%.

The effect on UVER, SW_{glo} and especially on SW_{dif} could be affected by the variations in the aerosol single scattering albedo

Table 4
Number of data, *N*, SZA(°), fit slope, *b* (Wm^{-2}), percentage change, *B* (%), correlation coefficient *r*, *p*-value, and 99% confidence interval obtained for the UVER, SW_{glo}, SW_{dif}, SW_{dir}, irradiances as functions of AOD_{550}, for different SZA values, for the period May to October 2012 at Marxaslokk, Malta.

Irradiance	*N*	SZA	*b* (Wm^{-2})	*B* (%)	*r*	*p*	i99%
UVER	61	20	−0.06	−28.12	−0.77	<0.001	(−0.878, −0.599)
	43	30	−0.07	−38.16	−0.75	<0.001	(−0.882, −0.516)
	42	40	−0.06	−42.01	−0.72	<0.001	(−0.869, −0.465)
	39	50	−0.04	−49.27	−0.76	<0.001	(−0.893, −0.520)
	37	60	−0.02	−47.30	−0.72	<0.001	(−0.875, −0.438)
	35	70	−0.01	−52.42	−0.80	<0.0001	(−0.913, −0.559)
SW_{glo}	61	20	−122	−13.46	−0.78	<0.001	(−0879, −0.602)
	43	30	−155	−18.65	−0.76	<0.001	(−0.887, −0.531)
	42	40	−158	−21.77	−0.75	<0.001	(−0.881, −0.506)
	39	50	−153	−26.13	−0.79	<0.001	(−0.908, −0.575)
	37	60	−138	−32.08	−0.79	<0.001	(−0.907, −0.555)
	35	70	−108	−41.41	−0.78	<0.001	(−0.907, −0.539)
SW_{dif}	61	20	287	222	0.88	<0.001	(0.769, 0.935)
	43	30	274	240	0.82	<0.001	(0.628, 0.914)
	42	40	271	238	0.83	<0.001	(0.649, 0.921)
	39	50	254	236	0.86	<0.001	(0.699, 0.938)
	37	60	198	210	0.80	<0.001	(0.571, 0.911)
	35	70	134	166	0.82	<0.001	(0.606, 0.924)
SW_{dir}	61	20	−409	−53	−0.87	<0.001	(−0.932, −0.759)
	43	30	−430	−60	−0.82	<0.001	(−0.916, −0.633)
	42	40	−429	−70	−0.82	<0.001	(−0.917, −0.634)
	39	50	−406	−85	−0.86	<0.001	(−0.937, −0.694)
	37	60	−336	−100	−0.82	<0.001	(−0.920, −0.608)
	35	70	−242	−135	−0.83	<0.001	(−0.929, −0.631)

(SSA) because the scatter radiation for a given AOD is lower when the SSA decrease (higher aerosol absorption); however this effect has not been taken into account due to the lack of SSA measurements.

Additional comparisons of results from other areas across the Mediterranean basin have been included. For instance Román et al. (2012) found a variation of −28.4% per unit of AOD_{440nm} in Spain for SW_{glo}, which concurs with the results obtained in Marsaxlokk, Malta. Moreover, aerosol attenuation is higher in global UVER than in global SW. Antón et al. (2011) at Granada, southeaster Spain observed a UVER reduction of (~25%) when AOD increases one unit. Di Sarra et al. (2002) at Lampedusa Island, (Central Mediterranean), Italy, estimated by a model that aerosol layer of optical depth 0.5 at 415 nm produces a reduction of the UVER irradiance as large as 25 and 27% at solar zenith angles of 30° and 60° respectively. Kazadzis et al. (2009) observed changes in the aerosol absorption properties at Tessaloniki, Greece, and a reduction of 15% in UV (325–340 nm) irradiance for a unit of aerosol optical depth was found. Esteve et al. (2009) analysed the effects of aerosols on UV erythemal in Valencia, Spain and the results showed that 70% of the variation in UV was determined by the variation of AOD at 500 nm. From the comparisons we can deduce that the results obtained at Marxaslokk are according with the obtained at the Mediterranean basin.

4.5. Ångström exponent effect

The Ångström exponent was seen to influence solar irradiance although it was also observed there is a correlation between the Ångström exponent and AOD_{550}. As a result, irradiance dependence on AOD_{550} must be removed. As with expression (5), UVER and SW were normalized for a fixed value of AOD_{550}, for example 0.2, using the following expression:

$$UVER_{AOD_{550}=0.2} = \left(1 - B_{AOD_{550}} \frac{0.2 - AOD_{550}}{100}\right) UVER \quad (6)$$

where $UVER_{AOD550=0.2}$ is the irradiance normalized to AOD_{550} with a value of 0.2; $B_{AOD_{550}}$ is the percentage changes shown in Table 4; and UVER is the measured irradiance. The same process was applied to SW_{glo}, SW_{dif} and SW_{dir} and their normalized values are plotted as a function of the Ångström exponent for different SZA values. Fig. 6 shows that solar UVER and global SW irradiance do not change with the Ångström exponent. The change and confidence intervals for Fig. 6 are shown in Table 5 where no variation proves statistically significant and, as a result, there is no direct dependence between irradiance and the Ångström exponent. Then, irradiances were then normalized to a higher AOD_{550} value of 0.8 to see whether irradiance is sensitive to the Ångström exponent. The new irradiances were calculated using Equation (6) and replacing 0.2 by 0.8. Fig. 7 shows the fitted results. The statistical results are summarised in Table 6. Here, variations are not significant, with UVER irradiance diminishing between −0.91% and −2.78% per unit of α. All changes for SW_{glo} irradiance are negative and none is statistically significant. Solar direct irradiance variations are negative and none statistically significant and their absolute values rise when SZA increases. When solar irradiances were normalized to an AOD_{550} value of 0.8, the Ångström exponent effect proved significant influence on SW_{dif} irradiance for SZA between 20° and 60°but the correlation is low. It means that α only influences irradiance if there is aerosol in the atmosphere, since if aerosol were not present

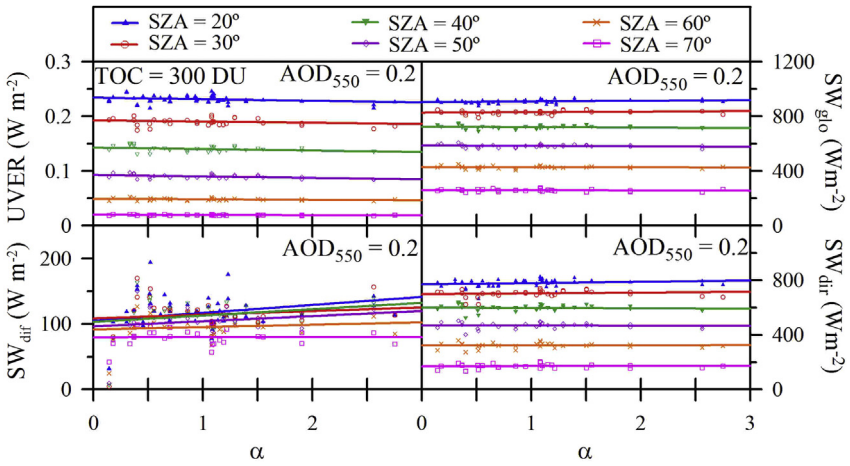

Fig. 6. UVER irradiance normalized to 300 DU (up right), SW_{glo} (up left), SW_{dif} (down left) and SW_{dir} (down-right) irradiance normalized to AOD_{550} 0.2 as a function of Ångström exponent (α), for different solar zenith angle, SZA, and cloudless days, during the period May to October 2012 at Marxaslokk, Malta.

Table 5
Number of data, *N*, SZA(°), fit slope, *b* (Wm^{-2}), percentage change, *B* (%), correlation coefficient *r*, *p*-value, and 99% confidence interval obtained for the UVER, SW_{glo}, SW_{dif}, SW_{dir}, irradiances as functions of Ångström exponent (AOD_{550} = 0.2) for different SZA values, during the period May to October 2012 at Marxaslokk, Malta.

Irradiance	*N*	SZA	*b* (Wm^{-2})	*B* (%)	*r*	*p*	i99%
UVER	61	20	0.0001	0.05	0.01	0.957	(−0.320, 0.332)
	43	30	0.0047	2.47	0.27	0.086	(−0.134, 0.590)
	42	40	0.0006	0.43	0.04	0.779	(−0.352, 0.427)
	39	50	0.0000	0.01	0.00	0.994	(−0.403, 0.405)
	37	60	0.0004	0.85	0.08	0.651	(−0.409, 0.442)
	35	70	0.0000	0.24	0.02	0.908	(−0.107, 0.514)
SW_{glo}	61	20	6.70	0.74	0.23	0.079	(−0.107, 0.515)
	43	30	16.61	2.00	0.46	0.002	(0.085, 0.716)
	42	40	3.43	0.47	0.11	0.504	(−0.300, 0.477)
	39	50	3.74	0.64	0.14	0.410	(−0.285, 0.512)
	37	60	4.88	1.14	0.19	0.259	(−0.244, 0.561)
	35	70	1.32	0.51	0.06	0.749	(−0.379, 0.471)
SW_{dif}	61	20	9.22	8.18	0.13	0.320	(−0.205, 0.437)
	43	30	−2.82	−2.60	−0.04	0.780	(−0.423, 0.348)
	42	40	1.93	1.79	0.04	0.822	(−0.360, 0.421)
	39	50	2.38	2.37	0.05	0.767	(−0.363, 0.445)
	37	60	−5.43	−5.88	−0.13	0.450	(−0.516, 0.303)
	35	70	−3.05	−3.94	−0.10	0.556	(−0.507, 0.338)
SW_{dir}	61	20	26.36	3.38	0.38	0.003	(0.061, 0.627)
	43	30	42.18	5.93	0.48	0.001	(0.122, 0.734)
	42	40	18.71	3.09	0.25	0.105	(−0.152, 0.586)
	39	50	18.77	3.98	0.30	0.062	(−0.118, 0.629)
	37	60	20.42	6.22	0.34	0.041	(−0.090, 0.661)
	35	70	15.86	9.08	0.32	0.064	(−0.127, 0.654)

Table 6
Number of data, *N*, SZA(°), fit slope, *b* (Wm^{-2}), percentage change, *B* (%), correlation coefficient *r*, *p*-value, and 99% confidence interval obtained for the UVER, SW_{glo}, SW_{dif}, SW_{dir}, irradiances as functions of Ångström exponent (AOD_{550} = 0.8) for different SZA values, for the period May to October 2012 at Marxaslokk, Malta.

Irradiance	*N*	SZA	*b* (Wm^{-2})	*B* (%)	*r*	*p*	i99%
UVER	61	20	−0.0018	−0.93	−0.13	0.307	(−0.439, 0.201)
	43	30	0.0011	0.78	0.08	0.606	(−0.315, 0.452)
	42	40	−0.0010	−0.91	−0.09	0.559	(−0.466, 0.309)
	39	50	−0.0014	−2.25	−0.21	0.200	(−0.566, 0.213)
	37	60	−0.0004	−1.24	−0.11	0.533	(−0.499, 0.323)
	35	70	−0.0004	−2.78	−0.22	0.202	(−0.591, 0.226)
SW_{glo}	61	20	4.40	0.53	0.16	0.214	(−0.173, 0.463)
	43	30	12.08	1.64	0.37	0.014	(−0.017, 0.662)
	42	40	0.94	0.15	0.03	0.834	(−0.362, 0.418)
	39	50	0.42	0.09	0.02	0.914	(−0.390, 0.420)
	37	60	0.90	0.26	0.04	0.802	(−0.379, 0.450)
	35	70	−2.46	−1.26	−0.13	0.444	(−0.530, 0.310)
SW_{dif}	61	20	−77.91	−27.32	−0.56	0.000	(−0.750, −0.289)
	43	30	−93.58	−34.26	−0.63	<0.001	(−0.820, −0.329)
	42	40	−52.55	−19.44	−0.46	0.002	(−0.722, −0.086)
	39	50	−53.34	−21.10	−0.52	0.001	(−0.761, −0.140)
	37	60	−49.38	−23.42	−0.54	0.001	(−0.778, −0.156)
	35	70	−29.70	−18.82	−0.51	0.002	(−0.768, −0.105)
SW_{dir}	61	20	−3.42	−0.64	−0.06	0.625	(−0.382, 0.268)
	43	30	5.01	1.11	0.08	0.623	(−0.318, 0.450)
	42	40	−5.36	−1.54	−0.10	0.518	(−0.474, 0.300)
	39	50	−12.13	−5.32	−0.26	0.115	(−0.599, 0.166)
	37	60	−12.80	−10.08	−0.28	0.092	(−0.623, 0.152)
	35	70	−18.09	−61.10	−0.42	0.011	(−0.719, 0.005)

it would make no sense to talk of a variation in AOD with wavelength which is what α represents. Therefore, the higher the $AOD_{550,}$ the greater the amount of aerosol in the atmosphere and the greater the influence of α. This is why its effect is more significant for an AOD_{550} of 0.8 than 0.2.

5. Conclusions

Recorded data of erythemal and total shortwave cloud-free irradiance (global, diffuse and direct) and atmospheric compounds from the campaign carried out at Marsaxlokk, Malta, from 24 May to 15 October 2012 are presented. UVER and total solar irradiance dependence on astronomical factors and atmospheric compounds have been quantified and their statistical significance has also been evaluated and tested. UVER irradiance depends on SZA cosine by a power law, with global and direct solar irradiance showing a linear dependence.

For different SZA values, the effect of total ozone column on UVER is shown and irradiance UVER levels are reduced in the range −0.24% DU^{-1} and −0.32% DU^{-1} varying with SZA. Water vapour column reduces global SW irradiance between −2.44% cm^{-1} and −4.53% cm^{-1}, these values rising when SZA increases from 20° to 70°, and solar diffuse irradiance increasing with *w* between 42.15% cm^{-1} and 20.30% cm^{-1} from low to high solar zenith angles. It has been observed that SW_{dif} does not increase with *w* when AOD_{550} is fixed. In addition, the increase in the diffuse component was due to the dust episodes in Malta whose synoptic conditions also increase water vapour and it makes possible the hygroscopic growth of aerosols and as consequence the increases of SW_{dif}.

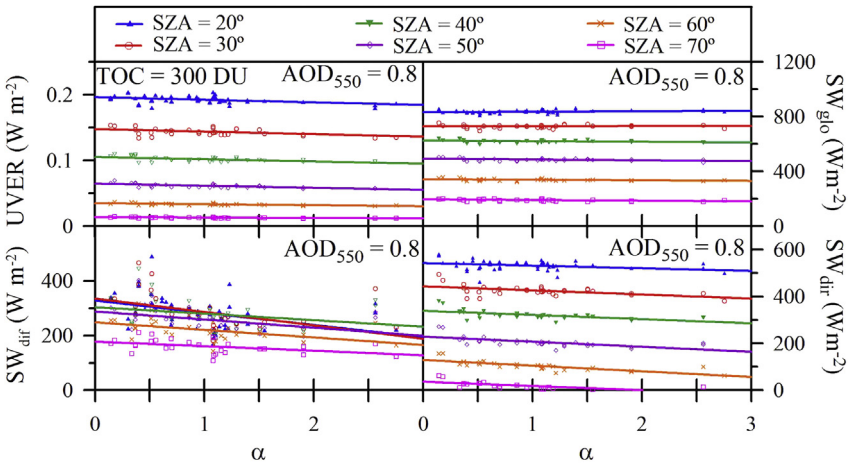

Fig. 7. UVER irradiance normalized to 300 DU (up left), SW_{glo} (up left), SW_{dif} (down left) and SW_{dir} (down-right) normalized to AOD_{550} 0.8 as a function of Ångström exponent, α, for different solar zenith angles, SZA, and cloudless days, during the period May to October 2012 at Marxaslokk, Malta.

Table 4 shows one AOD_{550} unit reduces more UVER (from −28.12% to −52.42%) irradiance than global SW (from −13.46% to −41.41%). The Ångström exponent causes variation in diffuse solar irradiance only when AOD_{550} is high, and not in global SW.

Atmospheric compounds are known to attenuate solar radiation through the atmosphere and a quantitative knowledge is important for modelling and forecasting solar radiation under cloudless sky conditions. In addition, solar resource data and radiation modelling will improve their accuracy if attenuation factors are available.

Acknowledgements

The authors gratefully acknowledge the support of the Spanish Research and Economy Ministry through Projects CGL2010-25385 and CGL2010-12410-E. We would like to thank the National Aeronautics and Space Administration and the European Space Agency for MODIS, OMI and GOME-2 data products. The authors also thank the principal investigator, Dr D. Meloni and her team for making the use of AERONET data information possible and for their efforts in establishing and maintaining the AERONET station at Lampedusa, Italy. The authors gratefully thank the use of HYSPLIT model (Hybrid Single Particle Lagrangian Integrated Trajectory Model) and the sounding from Wyoming University Atmospheric Science http://ready.arl.noaa.gov/HYSPLIT.php and http://weather.uwyo.edu/upperair/sounding.html. Roberto Román wishes to thank the University of Valladolid for the support provided through the PIF-UVa grant.

References

Antón, M., Serrano, A., Cancillo, M.L., Gracia, A., 2008. Total ozone and solar erythemal irradiance in southwestern Spain: day-to-day variability and extreme episodes. Geophys. Res. Lett. 35, L20804. http://dx.doi.org/10.1029/2008GL035290.

Antón, M., Gil, J.E., Fernández-Gálvez, J., Lyamani, H., Valenzuela, A., Foyo-Moreno, I., Olmo, F.J., Alados-Arboledas, L., 2011. Evaluation of the aerosol forcing efficiency in the UV erythemal range at Granada, Spain. J. Geophys. Res. 116, D20214. http://dx.doi.org/10.1029/2011JD016112.

Badarinath, K.V.S., Kharol, S.K., Kaskaoutis, D.G., Kambezidis, H.D., 2007. Influence of atmospheric aerosols on solar spectral irradiance in an urban area. J. Atmos. Sol. Terr. Phys. 69, 589–599. http://dx.doi.org/10.1016/j.jastp.2006.10.010.

Batlles, F.J., Olmo, F.J., Alados-Arboledas, L., 1995. On shadowband correction methods for diffuse irradiance measurements. Sol. Energy 54, 105–114.

Bilbao, J., de Miguel, A., 2013. Contribution to the study of UV-B solar radiation in Central Spain. Renew. Energy 53, 79–85. http://dx.doi.org/10.1016/j.renene.2012.10.055.

Bilbao, J., Miguel, A., Franco, J.A., Ayuso, A., 2004. Test reference year generation and evaluation methods in the continental Mediterranean area. J. Appl. Meteorol. 43, 390–400. http://dx.doi.org/10.1175/1520-0450(2004)0432.0.CO;2.

Bilbao, J., Román, R., de Miguel, A., Mateos, D., 2011. Long-term solar erythemal UV irradiance data reconstruction in Spain using a semiempirical method. J. Geophys. Res. 116, D22211. http://dx.doi.org/10.1029/2011JD015836.

C.I.E., 1998. Commission Internationale de l'Eclairage, Erythema Reference Action Spectrum and Standard Erythema Dose. CIE S007E-1998. CIE Central Bureau, Vienna, Austria.

De Miguel, A., Bilbao, J., 2005. Test reference year generation from meteorological and simulated solar radiation data. Sol. Energy 78, 695–703. http://dx.doi.org/10.1016/j.solener. 2004 .09 .015.

De Miguel, A., Román, R., Bilbao, J., Mateos, D., 2011. Evolution of erythemal and total shortwave solar radiation in Valladolid, Spain: effects of atmospheric factors. J. Atmos. Sol. Terr. Phys. 73, 578–586. http://dx.doi.org/10.1016/jastp.2010.11.021.

Di Sarra, A., Di Dorio, T., Cacciani, M., Fiocco, G., Fuá, D., 2001. Saharan dust profiles measured by lidar at Lampedusa. J. Geophys. Res. 106, 10,335–10,347. http://dx.doi.org/10.1029/2000JD900734.

Di Sarra, A., Cacciani, M., Chamard, P., Cornwall, C., DeLuisi, J.J., Di Dorio, T., Disterhoft, P., Fiocco, G., Fuá, D., Monteleone, F., 2002. Effects of dessert dust and ozone on the ultraviolet irradiance at the Mediterranean island of Lampedusa during PAUR II. J. Geophys. Res. 107 (D18), 8135. http://dx.doi.org/10.1029/2000JD000139.

Dubrovsky, M., 2000. Analysis of UV-B irradiances measured simultaneously at two stations in the Czech-Republic. J. Geophys. Res. 105, 4907–4913. http://dx.doi.org/10.1029/1999JD900374.

Esteve, A.R., Martinez-Lozano, J.A., Marin, M.J., Estelles, V., Tena, F., Utrillas, M.P., 2009. The influence of ozone and aerosols on the experimental values of UV erythemal radiation at ground level in Valencia. Int. J. Climatol. 29, 2171–2182. http://dx.doi.org/10.1002/joc. 1847.

Fioletov, V.E., McArthur, L.J.B., Mathews, T.W., Marrett, L., 2009. On the relationship between erythemal and vitamin D action spectrum weighted ultraviolet radiation. J. Photochem. Photobiol. B Biol. 95, 9–16. http://dx.doi.org/10.1016/j.jphotobiol. 2008.11.014.

Gueymard, C.A., 2012. Temporal variability in direct and global irradiance at various time scales as affected by aerosols. Sol. Energy 86, 3544–3553. http://dx.doi.org/10.1016/j.solener. 2012. 01. 013.

Hülsen, G., Gröbner, J., 2007. Characterization and calibration of ultraviolet broadband radiometers measuring erythemally weighted irradiance. Appl. Opt. 46 (23), 5877–5886.

Iqbal, M., 1983. An Introduction to Solar Radiation. Academic Press, New York.

Kaufman, Y.J., Tanré, D., Remer, L.A., Vermote, E.F., Chu, A., Holben, B.N., 1997. Operational remote sensing of tropospheric aerosol over land from EOS moderate resolution imaging spectroradiometer. J. Geophys. Res. 102, 17,051–17,076.

Kazadzis, S., Kouremeti, N., Bais, A., Kazantzidis, A., Meleti, C., 2009. Aerosol forcing efficiency in the UVA region from spectral solar irradiance measurements at an urban environment. Ann. Geophys. 27, 2515–2522. http://dx.doi.org/10.5194/angeo-27-2515-2009.

Koepke, P., Reuder, J., Schwander, H., 2002. Solar UV radiation and its variability due to the atmospheric components. Recent Res. Dev. Photochem. Photobiol. 6, 11–34.

Liu, S.C., Mckeen, S.A., Madronich, S., 1991. Effect of anthropogenic aerosols on biologically active ultraviolet radiation. Geophys. Res. Lett. 18, 2265–2268. http://dx.doi.org/10.1029/91GL02773.

Madronich, S., McKenzie, R.L., Bjorn, L.O., Caldwell, M.M., 1998. Changes in biologically active ultraviolet radiation reaching the Earth's surface. J. Photochem. Photobiol. B Biol. 46, 5–19.

Mateos, D., Bilbao, J., Kudish, A.I., Parisi, Carbajal, G., Di Sarra, A., Román, R., de Miguel, A., 2013. Validation of satellite erythemal radiation retrievals using ground-based measurements in five countries. Remote Sens. Environ. 128, 1–10. http://dx.doi.org/10.1016/j.rse.2012.09.015.

Mateos, D., Pace, G., Meloni, D., Bilbao, J., Di Sarra, A., de Miguel, A., Casasanta, G., Min, Q., 2014a. Observed influence of liquid cloud microphysical properties on ultraviolet surface radiation. J. Geophys. Res. Atmos. 119 http://dx.doi.org/10.1002/2013JD020309.

Mateos, D., Di Sarra, A., Bilbao, J., Meloni, D., Pace, G., de Miguel, A., Casasanta, G., 2014b. Spectral attenuation of global and diffuse UV irradiance and actinic flux by clouds. Q. J. R. Meteorol. Soc. http://dx.doi.org/10.1002/qj.2341.

McKenzie, R.L., Matthews, W.A., Johnston, P.V., 1991. The relationship between UV and ozone, derived from spectral irradiance measurements. J. Geophys. Res. 18, 2269–2272.

McKinlay, A.F., Diffey, B.L., 1987. A Reference Action Spectrum for Ultraviolet Induced Erythema in Human Skin, vol. 6. Commission Internationale de l' Eclairage (CIE), pp. 17–22.

Meloni, D., Marenco, F., Di Sarra, A., 2003. Ultraviolet radiation and aerosol monitoring at Lampedusa, Italy. Ann. Geophys. 46, 373–383.

Pace, G., Di Sarra, A., Meloni, D., Piacentino, S., Chamard, P., 2006. Aerosol optical properties at Lampedusa (Central Mediterranean). 1. Influence of transport and identification of different aerosol types. Atmos. Chem. Phys. 6, 697–713. http://dx.doi.org/10.5194/acp-6-697-2006, 2006.

Papadimas, C.D., Hatzianastassiou, N., Matsoukas, C., Kanakidou, M., Mihalopoulos, N., Vardavas, I., 2012. The direct effect of aerosols on solar radiation over the broader Mediterranean basin. Atmos. Chem. Phys. 12, 7165–7185. http://dx.doi.org/10.5194/acp-12-7165-2012.

Perez, R., Ineichen, P., Seals, R., 1990. Modelling daylight availability and irradiance componentsfrom direct and global irradiance. Sol. Energy 44, 271–289.

Reda, I., Andreas, A., 2003. Solar Position Algorithm for Solar Radiation Application. National Renewable Energy Laboratory (NREL). Technical report NREL/TP-560-34302. Revised January 2008.

Román, R., Mateos, D., de Miguel, A., Bilbao, J., Pérez-Burgos, A., Rodrigo, R., Cachorro, V.E., 2012. Atmospheric effects on the ultraviolet erythemal and total shortwave solar radiation in Valladolid, Spain. Opt. Pura Apl. 45, 17–21. http://dx.doi.org/10.7149/OPA.45.1.17.

Román, R., Antón, M., Valenzuela, A., Gil, J.E., Lymani, H., de Miguel, A., Olmo, F.J., Bilbao, J., Alados-Arboledas, L., 2013. Evaluation of the desert dust effects on global, direct and diffuse spectral ultraviolet irradiance. Tellus B 65, 19578. http://dx.doi.org/10.3402/tellusb.v65i0.19578.

Román, R., Bilbao, J., de Miguel, A., 2014. Uncertainty in water vapor column, aerosol optical depth and Angström Exponent, and its effect on radiative transfer simulations in the Iberian Peninsula. Atmos. Environ. 89, 556–569. http://dx.doi.org/10.1016/j.atmosenv.2014.02.027.

Seckmeyer, G., Mayer, B., Bernhard, G., Erb, R., Albold, A., Jäger, H., Stockwell, W.R., 1997. New maximum UV irradiance levels observed in Central Europe. Atmos. Environ. 31, 2971–2976. http://dx.doi.org/10.1016/S1352-2310(97)00104-0.

Siani, A.M., Casale, G.R., Galliani, A., 2002. Investigation on a low ozone episode at the end of November 2000 and its effect on ultraviolet radiation. Opt. Eng. 41, 3082–3089.

Stick, C., Krüger, K., Schade, N.H., Sandmann, H., Macke, A., 2006. Episode of unusual high solar ultraviolet radiation over central Europe due to dynamical reduced total ozone in May 2005. Atmos. Chem. Phys. 6, 1771–1776. http://dx.doi.org/10.5194/acp-6-1771-2006.

UNEP (United Nations Environment Programme), 2010. Environmental Effects of Ozone Depletion and its Interactions with Climate Change: 2010 Assessment. ISBN 92-807-2312-X.

Vilaplana, J.M., Cachorro, V.E., Sorribas, M., Luccini, E., de Frutos, A.M., Berjón, A., de la Morena, B., 2009. Modified calibration procedures for a Yankee environmental system UVB-1 biometer based on spectral measurements with a brewer spectrophotometer. Photochem. Photobiol. 82, 508–514.

Webb, A.R., 2006. Who, what, where and when-influences on cutaneous vitamin D synthesis. Prog. Biophys. Mol. Biol. 92, 17–25.

Webb, A.R., Slaper, H., Koepke, P., Schmalwieser, A.W., 2011. Know your standard: clarifying the CIE erythema action spectrum. Photochem. Photobiol. 87, 483–486.

WMO, 2010. WMO/UNEP Assessment, Scientific Assessment of Ozone Depletion: 2010. World Meteorological Organization Global Ozone Research and Monitoring Project Report No. 52. Genève, Switzerland.